Proceedings of the 20th National and 9th International ISHMT-ASME Heat and Mass Transfer Conference
January 4-6, 2010, Mumbai, India

10HMTC129

PERFORMANCE ANALYSIS OF METAL HYDRIDE BASED COOLING SYSTEMS

A. Satheesh
Department of Mechanical Engineering
Indian Institute of Technology Guwahati
Guwahati – 781039, India
satheesh@iitg.ernet.in

P. Muthukumar
Department of Mechanical Engineering
Indian Institute of Technology Guwahati
Guwahati – 781039, India
pmkumar@iitg.ernet.in

Anupam Dewan*
Department of Mechanical Engineering
Indian Institute of Technology Guwahati
Guwahati – 781039, India
adewan@iitg.ernet.in

ABSTRACT

This paper presents a numerical investigation of a single-stage single-effect metal hydride based cooling system working with two different metal hydride pairs, namely, $LmNi_{4.91}Sn_{0.15}$ / $Ti_{0.99}Zr_{0.01}V_{0.43}Fe_{0.09}Cr_{0.05}Mn_{1.5}$ (1^{st} alloy pair) and $LaNi_{4.61}Mn_{0.26}Al_{0.13}$ / $La_{0.6}Y_{0.4}Ni_{4.8}Mn_{0.2}$($2^{nd}$ alloy pair). The influence of operating parameters such as heat source, heat sink and refrigeration temperatures (T_H, T_M and T_C), and bed parameters such as thermal conductivity and bed thicknesses on system performance is predicted. The unsteady, two-dimensional, mathematical model in an annular cylindrical configuration is solved numerically for predicting the conjugate heat and mass transfer characteristics between coupled reactors by using the fully implicit finite volume method (FVM). Numerical results are validated with the experimental data reported in the literature. Results show that for a given heat sink and refrigeration temperatures, COP of the system, specific cooling power (SCP) and the amount of hydrogen exchange between the paired reactors are found to increase with heat source temperature. For a given operating conditions and reactor geometry, COP and SCP of $LmNi_{4.91}Sn_{0.15}$ / $Ti_{0.99}Zr_{0.01}V_{0.43}Fe_{0.09}Cr_{0.05}Mn_{1.5}$ and $LaNi_{4.61}Mn_{0.26}Al_{0.13}$ / $La_{0.6}Y_{0.4}Ni_{4.8}Mn_{0.2}$ hydride pairs are found to be 0.543, 53.25 W/kg and 0.43, 56.2 W/kg, respectively.

NOMENCLATURE

A	Surface area [m^2]
C	Reaction rate constant [s^{-1}]
C_p	Specific Heat [J/kg-K]
COP	Coefficient of performance
E	Activation energy [J/mol H_2]
k	Thermal conductivity [W/m-K]
K	Permeability [m^2]
m	Mass [kg]
M_g	Molecular weight of the hydrogen gas [kg/kmol]
n	No. of moles of hydrogen [mol]
P	Pressure [bar]
q_o	Specific alloy output [W/kg]
r	Radius of the reactor [m]
R_u	Universal gas constant [J/mol-K]
t	Time (s)
T	Temperature (K)
u	Velocity (m/s)
U	Over all heat transfer coefficient [W/m^2-K]
V	Volume (m^3)
X	Concentration
Z	Compressibility factor

Greek symbols

Φ, Φ_o	Slope factor constants.
β	Hysteresis factor
ΔH	Enthalpy of formation [J/mol H_2]
ΔS	Enthalpy of formation [J/mol H_2-K]
ρ	Density [kg/m^3]
ε	Porosity
μ	Dynamic viscosity [kg/m-s]

Subscripts

a	absorption
A	high temperature reactor
B	low temperature reactor
C	refrigeration
d	desorption
e	effective
f	fluid, final
fi	heat transfer fluid inlet
fo	heat transfer fluid outlet
g	gas
h	metal hydride
H	heat source
m	metal
M	heat sink
max	maximum
min	minimum
r	reactor
ss	Saturated solid

***Present address: Department of Applied Mechanics,** IIT Delhi, Hauz Khas, New Delhi – 110016, India

INTRODUCTION

Due to the absence of harmful chloro-fluro-carbon (CFCs) and a substantial reduction of CO_2 emissions, thermally driven sorption cooling systems have received much attention in the recent times. Among these systems, metal hydride based heating and cooling systems deserve attention due to their compactness, high specific cooling power (SCP) and various operating and impressive environmental benefits. Since past three decades, many authors have reported the development of metal hydride heat pump (MHHP) systems for various applications such as refrigeration, air-conditioning, etc. [1-11]. Gopal and Murthy [1] numerically investigated a single-stage metal hydride cooling system working with ZrMnFe/$MmNi_{4.5}Al_{0.5}$ hydride alloy pair using a one-dimensional model. They studied the performance characteristics of the system by varying the bed thicknesses, thermal conductivities and overall heat transfer coefficients. They obtained the COP of the system from 0.45 to 5.0 for the operating temperatures range of T_H = 120 to 155°C, T_M = 20 to 30°C and T_C = 0 to 10°C. However, their numerical model was limited to thin beds and did not include the effect of convection heat transfer in the energy equation. Subsequently, the same research group conducted experiments [2] with the same metal hydride pair for comparing their numerical results. Fedorov et al. [3] presented the simulation of a MHHP system using $LaNi_{4.5}Al_{0.25}H_x$ / $TiFe_{0.8}Mn_{0.2}H_y$ hydride pair without considering the effect of hysteresis and plateau slope on the pressure concentration isotherm (PCT). Jang et al. [4] developed an unsteady, one-dimensional mathematical model of MHHP system using $Zr_{0.9}Ti_{0.1}Cr_{0.9}Fe_{1.1}$ / $Zr_{0.9}Ti_{0.15}Cr_{0.6}Fe_{1.45}$ the hydride pair. Qin et al. [5] conducted experiments using $LaNi_{4.61}Mn_{0.26}Al_{0.13}$ / $La_{0.6}Y_{0.4}Ni_{4.8}Mn_{0.2}$ hydride pair at 120 to 200°C / 20 to 50°C /-10 to 0°C ($T_H/T_M/T_C$) temperature range for air-conditioner using exhaust gas from an automobile. The COP and SCP of the system increased with source temperature from 0.12 and 61 W at 115°C to 0.26 and 238 W at 150°C. Ni and Liu [6] tested a metal hydride cooling system working with the same hydride pair used by Qin et al [5]. They observed a large deviation between the static and dynamic van't Hoff diagrams. For the given operating temperatures of 150°C/30°C/20°C, the maximum COP and cooling rate of about 0.3 and 240W were achieved.

Recently, Payá et al. [7] carried out the zero-dimensional mathematical model working with $LmNi_{4.91}Sn_{0.15}$ / $Ti_{0.99}Zr_{0.01}V_{0.43}Fe_{0.09}Cr_{0.05}Mn_{1.5}$ hydride pairs. For the given operating temperature limits of 130°C/35°C/20°C, the maximum cooling power and the system COP were found to be approximately 736 W and 0.22, respectively. Their numerical results were validated with their own experimental data reported in the literature [8]. Mellouli et al. [9] numerically investigated the performance of MHHP employing $MmNi_{4.5}Al_{0.5}$ / $MmNi_{4.2}Al_{0.1}Fe_{0.7}$ hydride pair. Depending on the operating temperature range of 325 to 340 K / 273 to 293 K / 250 to 265 K; the system COP was varied from 0.45 to 0.5 and the SCP was increased up to 120 W/kg of alloy. In a recent study, Satheesh et al. [10] reported a transient, two-dimensional, mathematical model working with $MmNi_{4.6}Al_{0.4}$ / $MmNi_{4.6}Fe_{0.4}$ hydride alloy pair. The effects of various operating and bed parameters on COP and SCP were investigated for both constant wall temperature and variable wall temperature convective boundary conditions. The computations reveal that the difference in cycle times for the constant and variable wall temperature boundary conditions was approximately 5 min. Hence in the present paper, the variable wall temperature condition is adopted for the further mathematical modeling of the heat pump system. The literature survey shows that the numerical studies on MHHP systems are restricted to zero-dimensional [7] and one-dimensional models without considering the effect of convection in the energy equation [1, 4]. However, the metal hydride cooling system is not yet commercialized due to poor coupled heat and mass transfer characteristics of the powder metal hydride bed. Recently it has gained importance and has the potential for practical applications in some niche areas. Therefore in the present paper, the unsteady, two-dimensional mathematical model is solved to predict the performance of metal hydride cooling system for the selected hydride pairs. The present study includes the effect of convection and variation in the cooling fluid temperature along the axial direction on the performance. Further the effect of hysteresis and plateau slope are determined from the experimental results reported in the literature [5, 7] for the selected alloy pairs.

SELECTION OF HYDRIDE ALLOY PAIRS

The performances (COP and SCP) of MHHP system greatly depends on the proper selection of alloy within its operating range. The desirable properties of the hydriding alloy for achieving high COP and SCP are: the hydrogen exchange between the paired reactors should be high enough, high enthalpy of formation, low specific heat, high thermal conductivity and fast reaction kinetics, favorable equilibrium pressures, low hysteresis, flat plateau, simple activation process and minimum degradation after cyclic operation and long life. Table 1 shows the enthalpy and entropy of formations of the selected metal hydride pair during both absorption and desorption processes.

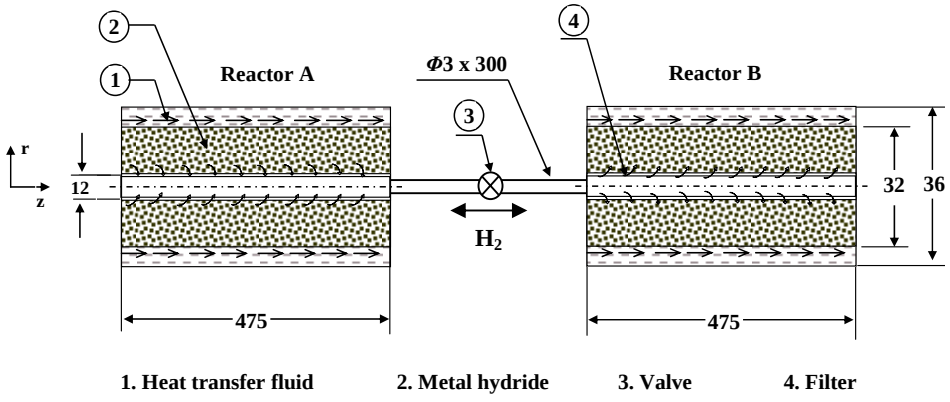
Table 1. ENTHALPY AND ENRTOPY OF FORMATION FOR THE SELECTED HYDRIDE PAIRS

Alloy pairs	ΔH (kJ/mol H_2)		ΔS (kJ/mol H_2 K)	
	Abs.	Dbs.	Abs.	Dbs.
$LaNi_{4.61}Mn_{0.26}Al_{0.13}$ (A)	-36.9	-37.6	-109.7	-108.2
$La_{0.6}Y_{0.4}Ni_{4.8}Mn_{0.2}$ (B)	-26.9	-26.6	-102.3	-97.4
$LmNi_{4.91}Sn_{0.15}$ (A)	-27.2	-32.4	-103.1	-112.8
$Ti_{0.99}Zr_{0.01}V_{0.43}Fe_{0.09}Cr_{0.05}Mn_{1.5}$ (B)	-20.0	-25.5	-97.0	-110.9

NUMERICAL MODEL

The physical model and the operating principle for the single stage MHHP has been described already in the previous papers [10, 11]. Fig.1 shows the schematic of coupled metal hydride reactors. Each reactor is of 475 mm length and 36 mm outer diameter. The innermost tube serves as the hydrogen filter of 12 mm outer diameter and the heat transfer fluid flows in the outer most peripheral tube of 1.0 mm gap. These two reactors are coupled by a connecting tube of 300 mm length and 3 mm inner diameter. During the entire process, the gas pressure drop in the connecting tube is calculated for the given operating condition and it is negligible. Hydride masses are calculated from the free volume of the reactor vessel (3.283×10^{-4} m^3) and hydride packing density (ρ) with a constant porosity (ε = 0.5).

Fig. 2 shows the operating cycle of a single stage MHHP working with $LaNi_{4.61}Mn_{0.26}Al_{0.13}$ / $La_{0.6}Y_{0.4}Ni_{4.8}Mn_{0.2}$ hydride pair. It consists of a total of four consequent processes which include two hydrogen transfer processes (*ab* and *cd*) and two heat transfer processes (*bc* and *da*).



All dimensions are in mm (not to scale)

Figure 1. SCHEMATIC OF COUPLED METAL HYDRIDE REACTORS.

During the first process, hydrogen is desorbed from high temperature hydride (regeneration alloy) by utilizing the low grade energy at temperature above 120°C (T_H). The desorbed hydrogen is acquired by low temperature metal hydride (refrigeration alloy) at medium temperature (T_M). In the third process, low temperature metal hydride is coupled to a high temperature hydride permitting energy to be extracted from the refrigerated space. Between these two processes there are transient periods, where two reactors are cooled down and heated up to the heat source temperature (T_H) to heat sink temperature (T_M) and heat sink temperature (T_M) to refrigeration temperature (T_C) and vice versa.

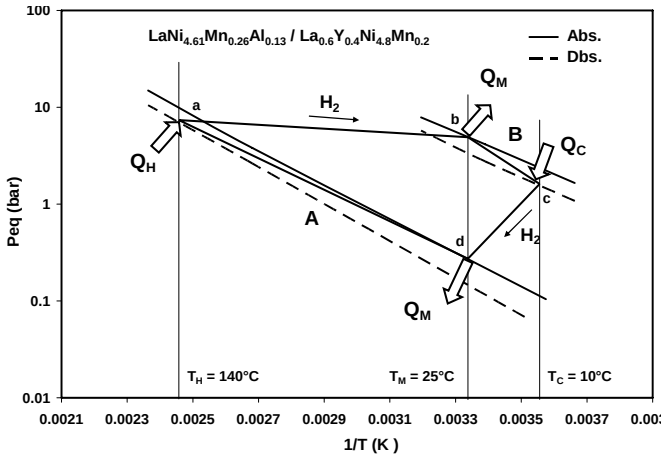


Figure 2. VAN'T HOFF PLOT FOR SINGLE-STAGE AND SINGLE-EFFECT METAL HYDRIDE HEAT PUMP.

Assumptions

The following assumptions are made in the modeling for single stage MHHP operation.

1. Initially, the two reactors (A and B) are in equilibrium with hydrogen gas.
2. Heat transfer in the reaction bed is transient, two-dimensional conduction and convection. The effect of radiation is negligible.
3. Thermo-physical properties of hydride alloys (thermal conductivity, enthalpy of formation and entropy of formation) are independent of the temperature, concentration and pressure.
4. Hydrogen gas pressure (P_g) and temperature (T_g) are assumed to be constant everywhere in the connecting pipe. But these are time dependent.
5. The reactors are assumed to be well insulated and no heat transfer takes place between them and surroundings.

PROBLEM FORMULATION AND SOLUTION

Initially ($t = 0$), the hydrogen gas in the connecting pipe is in equilibrium with the hydride beds. Hence, the gas pressure and temperature in the connecting pipe immediately after opening the valve are calculated from the following expressions

$$P_{g,P} = \frac{P_{g,A}V_A + P_{g,B}V_B}{V_A + V_B} \qquad T_{g,P} = \frac{n_A T_A + n_B T_B}{n_A + n_B} \tag{1}$$

where, $P_{g,A}$, V_A, $P_{g,B}$ and V_B are the hydrogen gas pressures and free volume of the reactors A and B, respectively. n_A, T_A, n_B and T_B are the number of moles of hydrogen gas and their corresponding temperatures in the reactors. $P_{g,A}$ and $P_{g,B}$ denote the gas pressures inside the reactors A and B. This can be calculated from the van't Hoff equation.

$$P_{eq,A} = \exp\left[\frac{\Delta H_A}{R_u T_A} - \frac{\Delta S_A}{R_u} + \left(\phi_A \pm \phi_{o,A}\right)\tan\left[\pi\left(\frac{X_A}{X_{f,A}} - \frac{1}{2}\right)\right] \pm \frac{\beta_A}{2}\right] \tag{2}$$

$$P_{eq,B} = \exp\left[\frac{\Delta H_B}{R_u T_B} - \frac{\Delta S_B}{R_u} + \left(\phi_B \pm \phi_{o,B}\right)\tan\left[\pi\left(\frac{X_B}{X_{f,B}} - \frac{1}{2}\right)\right] \pm \frac{\beta_B}{2}\right] \tag{3}$$

The number of moles of hydrogen in the reactors A and B are determined using the real gas equation.

$$n_A = \frac{P_A V_A}{Z R_u T_A} \qquad n_B = \frac{P_B V_B}{Z R_u T_B} \tag{4}$$

where, Z is the compressibility factor. It is a function of pressure and temperature [11]. Based on the experimental results, the second order polynomial fit was taken with high accuracy (correlation coefficient = 0.99). The constants and their corresponding values are reported in the literature [11]. This compressibility factor is valid in the pressure and temperature range of $0.1 < P < 10$ MPa and $280 < T < 428$ K, respectively. The number of moles of hydrogen (n_g), gas temperature (T_g) and gas pressure (P_g) in the connecting pipe at any time during hydrogen transfer processes are calculated using the following equations

$$n_{g,t+\delta t} = n_{g,t} + n_d - n_a \tag{5}$$

$$T_{g,t+\delta t} = \frac{\left(n_{g,t} - n_a\right)T_{g,a} + n_d T_{g,d}}{n_{g,t} - n_a + n_d} \tag{6}$$

$$P_{g,t+\delta t} = \frac{Zn_{g,t+\delta t} R_u T_{g,t+\delta t}}{V_A + V_B} \tag{7}$$

where, $n_{g,t}$ denotes the number of moles of hydrogen gas at the connecting pipe immediately after opening the valve (t = 0). n_a and n_d denote the number of moles of hydrogen gas absorbed and desorbed at the corresponding reactors during any time step, respectively.

Process ab (First Half Cycle)

As stated in the physical model, the two hydrogen transfer (*ab* and *cd*) and two heat transfer (*bc* and *da*) processes are estimated by simultaneously solving the continuity, momentum and energy equations in both the reactors. During the first half cycle, hydrogen (full hydride) is desorbed from the reactor A by taking the heat of desorption from the heat transfer fluid temperature (T_H) which is absorbed at reactor B by releasing the heat of absorption to the heat transfer fluid at medium temperature (T_M). The computational modeling of the above process is discussed below.

Reactor A (Desorption): Mass flux during the desorption of hydrogen is given by

$$m_A = C_d \exp\left(\frac{-E_d}{R_u T_A}\right)\left(\frac{P_{eq,A} - P_{g,t+\delta t}}{P_{eq,A}}\right)\rho_{m,A} \tag{8}$$

where, C_d and E_d denote the reaction rate constant and activation energy, respectively. These values are determined from the experimental results. $P_{eq,\ A}$, and $\rho_{m,\ A}$ are the equilibrium pressure at reactor A and the density of the metal hydride alloy at any given time step (t+δt), respectively. Assuming thermal equilibrium between the hydride bed and hydrogen, a combined energy equation is considered instead of separate equations for both solid and gases phases

$$\left(\rho C_p\right)_e \frac{\partial T}{\partial t} + \left(\rho C_p\right)_g \vec{u}.\nabla T = k\nabla^2 T - m_A\left[\frac{\Delta H}{M_g} - T\left(Cp_g - Cp_s\right)\right] \tag{9}$$

where,

$$\left(\rho C_p\right)_e = \left(\varepsilon \rho C_p\right)_g + \left((1-\varepsilon)\rho C_p\right)_s \tag{10}$$

and the effective thermal conductivity

$$k = \varepsilon k_g + (1-\varepsilon)k_s. \tag{11}$$

The hydrogen mass balance is expressed as

$$\varepsilon \frac{\partial\left(\rho_g\right)}{\partial t} + \nabla\left(\rho_g \overrightarrow{u_g}\right) = m_A. \tag{12}$$

where, ρ_g denotes the density of the hydrogen gas and it is determined using the real gas equation. Velocity of the hydrogen gas (u_g) is calculated using the Darcy's law

$$\vec{u}_g = -\frac{K}{\mu_g}\nabla P_g. \tag{13}$$

By substituting the density and velocity of the hydrogen gas in Eq. (12), the gas pressures inside the reactors are determined using the following equations

$$\begin{aligned}&\left(\frac{\varepsilon M_g}{ZR_u T}\right)\frac{\partial P_g}{\partial t} + \left(\frac{\varepsilon M_g P_g}{ZR_u}\right)\frac{\partial}{\partial t}\left(\frac{1}{T}\right) - \left[\frac{2a}{T}\left(1+P_g\right)\right]\frac{\partial^2 P_g}{\partial r^2} \\ &- \left[\frac{a}{T}\left(1+P_g\right)\right]\frac{\partial^2 P_g}{\partial z^2} - 2aP_g\frac{\partial P_g}{\partial r}\frac{\partial}{\partial r}\left(\frac{1}{T}\right) - aP_g\frac{\partial P_g}{\partial z}\frac{\partial}{\partial z}\left(\frac{1}{T}\right) \\ &- \frac{2aP_g}{rT}\frac{\partial P_g}{\partial r} = m_A\end{aligned} \tag{14}$$

where,

$$a = \frac{KM_g}{Z\mu_g R_u} \tag{15}$$

Here M_g denotes the molecular weight of hydrogen gas, K the coefficient of Darcy law and μ_g the dynamic viscosity of the gas.

Initial and boundary conditions: Initially at time t = 0, the reactors A and B are in equilibrium with hydrogen gas at their respective temperatures limits. Temperature and concentration of the reactor A are given by

$$\rho_{m,A}(z,r) = \rho_{ss}; T_{m,A}(z,r) = T_{g,A}(z,r) = T_H; X_A(z,r) = X_{\max}. \tag{16}$$

The left and right boundaries of the reactor are assumed to be adiabatic

$$\frac{\partial T}{\partial z}(z,r,t)_{z=0} = 0 \qquad \frac{\partial T}{\partial z}(z,r,t)_{z=Z} = 0 \tag{17}$$

and at the bottom wall (along the porous filter)

$$\frac{\partial T}{\partial r}(z,r,t)_{r=r_i} = 0 \qquad P_g(z,r_i,t) = P_g. \tag{18}$$

The cooling fluid flows through the outer peripheral tube and therefore the convective boundary condition is applied at the top boundary. The difference in the cycle time and the difference between constant wall convective boundary condition and the variable wall temperature condition was already presented in the literature [10, 11]. Therefore in the present work the variable outer wall temperature boundary condition is considered for modeling.

$$T_{fo} = T_{fi} + [T_{z,r_o,t} - T_{fi}]\left[1 - \exp\left(-\frac{UA}{m_f Cp_f}\right)\right]. \tag{19}$$

where, T_{fo} and T_{fi} are the heat transfer fluid temperature at outlet and inlet conditions. $T_{z,ro,t}$ denote the temperature of the hydride bed at the outer radius of the reaction bed.

Reactor B (Absorption): The mass flux of hydrogen during absorption is expressed as

$$m_B = C_a \exp\left(\frac{-E_a}{R_u T_B}\right)\ln\left(\frac{P_{g,t+\delta t}}{P_{eq,B}}\right)\left(\rho_{ss} - \rho_{m,B}\right) \tag{20}$$

where, ρ_{ss} and $\rho_{m,B}$ are the density of metal at saturated condition and density of metal in the reactor B at any given time (t). The temperature of the reactor B is updated by solving the following energy equation

$$\left(\rho C_p\right)_e \frac{\partial T}{\partial t} + \left(\rho C_p\right)_g \vec{u}.\nabla T = k\nabla^2 T + m_B\left[\frac{\Delta H}{M_g} - T\left(Cp_g - Cp_s\right)\right]. \tag{21}$$

The hydrogen mass balance during the absorption in the reactor B is expressed as

$$\varepsilon \frac{\partial(\rho g)}{\partial t} + \nabla\left(\rho g \overrightarrow{ug}\right) = -m_B. \quad (22)$$

Hydrogen gas pressure in the reactor B is found in the same way as for the reactor A using Eq. (14)

Initial and boundary conditions: The initial conditions of the reactor B at time t = 0 are given by Eq. (23). The boundary conditions are similar to those for reactor A.

$$\rho_{m,B}(z,r)=\rho_i;\ T_{m,B}(z,r)=T_{g,B}(z,r)=T_M;\ X_B(z,r)=X_{\min}. \quad (23)$$

Process *bc* (Sensible Cooling)

During this process, only the heat transfer takes place between the hydride bed and the heat transfer fluid. Therefore, the governing equations for reactors A and B become

$$\left(\rho C_p\right)_e \frac{\partial T}{\partial t} + \left(\rho C_p\right)_g \vec{u}.\nabla T = k\nabla^2 T. \quad (24)$$

The initial conditions of the sensible cooling processes are used as the final conditions of the previous desorption / absorption process.

Process *cd* (Second Half Cycle)

During this process, hydrogen is transferred from reactor B to reactor A at low pressure. The initial condition of this process is the final condition of the sensible cooling process of the respective reactors. The governing equations and boundary conditions used in this process are similar to those for the first half cycle.

Process *da* (Sensible Heating)

In this process, the reactors A and B are heated to temperatures T_H and T_M, respectively. The final condition of this process is the initial condition of the next cycle of process *ab*.

PERFORMANCE ANALYSIS

The performance of the single stage MHHP system is designated by the coefficient of performance and the specific cooling power. These quantities are defined as

$$COP = \frac{Q_C}{Q_H} \quad (25)$$

here (Q_C) denotes the net refrigeration effect obtained at low temperature alloy during second half cycle and Q_H the thermal heat input (Q_H) at high temperature alloy.

$$Q_C = n_{B,d}\,\Delta H_{B,d} - \left[\left(m_h + m_r\right) Cp_B \left(T_M - T_C\right)\right] \quad (26)$$

$$Q_H = n_{A,d}\,\Delta H_{A,d} - \left[\left(m_h + m_r\right) Cp_A \left(T_H - T_M\right)\right] \quad (27)$$

where, $n_{A,\,d}$, $\Delta H_{A,\,d}$, $n_{B,\,d}$ and $\Delta H_{B,\,d}$ denote the number of moles of hydrogen and enthalpy of formation during desorption processes in the corresponding reactors A and B. m_h and m_r are the mass of the hydride alloy and mass of the reactor. For, solving the mathematical modeling, this ratio is taken as 1:2.

$$q_o = \frac{Q_C}{m_B\, t} \quad (28)$$

where, t and m_B denote a complete cycle time and the mass of the hydride B (including the reactor mass), respectively.

The numerical solution of the present mathematical modeling is solved using fully implicit finite volume method using central difference scheme. This study is carried out with cylindrical configuration including the effect of convection in the energy equation and the hysteresis and plateau slope of the PCT were accounted. The coupled heat and hydrogen transfer processes (*ab* and *cd*) are assumed to be converged when the difference between the gas pressures of the respective reactors and combined gas pressure is less than 0.01 bar. The sensible heat transfer processes (*bc* and *da*) are assumed to be converged when the difference between the heat transfer fluid temperature and average bed temperature is less than 0.1°C. For the given reactor geometry, hydride packing density and hydrogen exchange capacity between the coupled reactors, the analysis has been carried out for 1.3 and 1.15 kg alloy masses (reactor A and B) for $LmNi_{4.91}Sn_{0.15}$ / $Ti_{0.99}Zr_{0.01}V_{0.43}Fe_{0.09}Cr_{0.05}Mn_{1.5}$ hydride pair and 1.15 kg mass in each reactor for $LaNi_{4.61}Mn_{0.26}Al_{0.13}$ / $La_{0.6}Y_{0.4}Ni_{4.8}Mn_{0.2}$. The end conditions of the sensible heating process are taken as the initial conditions of the first process for the next cycle.

RESULTS AND DISCUSSION

Performance analysis of a single-stage single-effect MHHP system working with $LmNi_{4.91}Sn_{0.15}$ / $Ti_{0.99}Zr_{0.01}V_{0.43}Fe_{0.09}Cr_{0.05}Mn_{1.5}$ and $LaNi_{4.61}Mn_{0.26}Al_{0.13}$ / $La_{0.6}Y_{0.4}Ni_{4.8}Mn_{0.2}$ hydride pairs are chosen for the present study. The operating temperatures, bed thickness and the effective thermal conductivity of metal hydride are varied over the specific range to study the system performance. Table 2 shows the design and operating data range used for the present analysis. The validation of the present mathematical model is compared with the experimental data reported in the literature [6], which is already presented in the earlier paper [10].

Table 2. DESIGN AND OPERATING DATA RANGE FOR THE SELECTED HYDRIDE PAIRS

S.No	Parameters	Alloy pair 1	Alloy pair 2
1	T_H (K)	160/130	170/140
2	T_M (K)	35/25	35/25
3	T_C (K)	20/10	20/10
4	k (W/mK)	1.6/12	1.6/12
5	r_o - r_i (mm)	7.5/12.5	7.5/12.5
6	Carnot COP	0.79	0.70
7	Max. COP	0.543	0.430

Fig. 3 and 4 show the effect of heat source and heat sink temperatures on system COP and hydrogen exchange between the coupled reactors during the first half cycle for $LmNi_{4.91}Sn_{0.15}$ / $Ti_{0.99}Zr_{0.01}V_{0.43}Fe_{0.09}Cr_{0.05}Mn_{1.5}$ and $LaNi_{4.61}Mn_{0.26}Al_{0.13}$ / $La_{0.6}Y_{0.4}Ni_{4.8}Mn_{0.2}$, respectively.

For a given heat sink temperature, amount of hydrogen transferred from the reactor A to B is found to increase with heat source temperatures. The increase in hydrogen transfer from reactor A to B during the first half cycle is limited to the heat sink temperature of 423 K and 433 K for the first and second alloy pairs, respectively. Therefore the maximum COP (0.543 and 0.43) is obtained at the corresponding temperature at lower heat sink temperature of 298 K, beyond which the increase in heat source

temperature gives adverse effect. This results show that the increase in COP with heat source temperature is due to the exchange of large quantity of hydrogen transferred between the coupled reactors. This is mainly due to the pressure differences existing between the reactors, when the heat source temperature is increased.

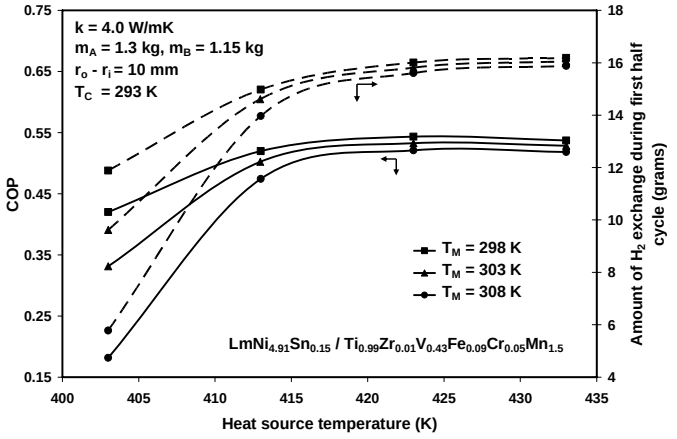


Figure 3. EFFECT OF T_H AND T_M ON COP AND H_2 EXCHANGE FOR 1ST ALLOY PAIR.

Figs. 3 and 4 show the maximum hydrogen transfer during the first half cycle is 16.18 and 12.75 grams for the first and second alloy pairs. The carnot COP of the system is found to be 0.79 and 0.7 for the first and second alloy pairs, respectively. For the heat sink temperature of 303 and 308 K, the amount of hydrogen exchange between the reactors during the first half cycle is found to be less than the maximum allowable limit of hydrogen transfer in the second half cycle from reactor B to A. Therefore, an increase in heat source temperature further increases the COP of the system to a limit. For a given heat source temperature, the amount of hydrogen transferred between the coupled reactor during the first half cycle is found to decrease with heat sink temperature. This is due to the driving force (difference in the equilibrium pressure) between reactors A and B.

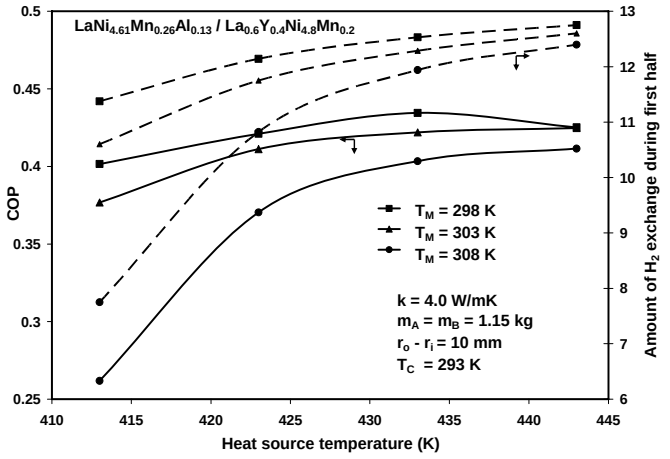


Figure 4. EFFECT OF T_H AND T_M ON COP AND H_2 EXCHANGE FOR 2ND ALLOY PAIR

Figs. 5 and 6 show the effect of heat source and heat sink temperatures on the total cycle time and specific cooling power output for the first and second alloy pairs of the MHHP system. For a given heat sink temperature, the cycle time is found to decrease with heat source temperatures. Decrease in the cycle time at higher heat source temperature is due to an increase in driving force between the reactors A and B. Decrease in cycle time significantly improves the specific cooling power. Apart from that, the increase in hydrogen exchange (with heat source temperature) between the reactors A and B during the first half cycle also increases the amount of heat extracted from the refrigerated space, when the hydrogen is desorbing from low temperature alloy during the second half cycle.

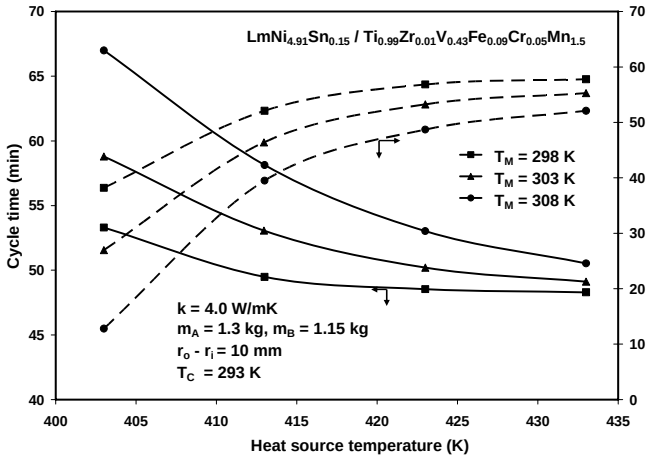


Figure 5. EFFECT OF T_H AND T_M ON CYLCE TIME AND SPECIFIC COOLING POWER FOR 1ST ALLOY PAIR

Fig. 5 shows that for a given heat sink temperature of 298 and 303 K, the increase in specific cooling power is significant for the heat source temperature of 423 K, beyond which the its effect is negligible. This is due to the amount of hydrogen exchanged between the reactors A and B.

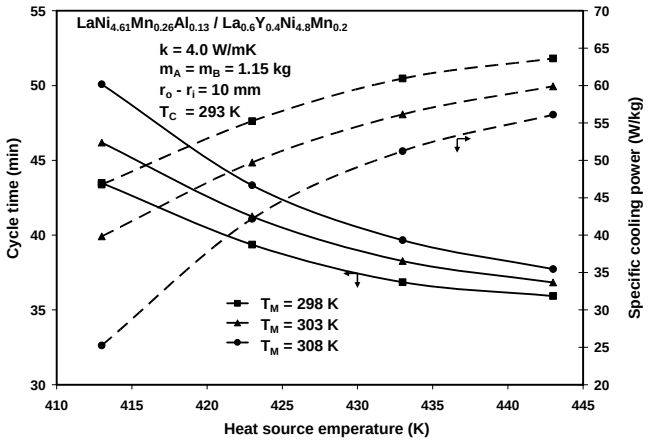


Figure 6. EFFECT OF T_H AND T_M ON CYLCE TIME AND SPECIFIC COOLING POWER FOR 2ND ALLOY PAIR

Fig.6 shows that for a given heat sink temperature of 298 K, the specific cooling power can be still improved by increasing the heat source temperature. But that is due to decrease in cycle time. Since, the COP is found to increase with heat source temperature of 423 K. beyond which it makes the adverse effect. Hence for a given operating temperature of 423/298/293 K the optimum performance of the MHHP system for the first alloy pair is observed. Similarly, 433/298/293 K is preferred for the second alloy pair. Fig. 7 shows the effect of heat source and refrigeration temperature on system COP for the selected alloy pairs. It is observed that for the given heat source temperature, the COP of the system is found to increase with refrigeration temperature. For the given refrigeration temperature, the COP of the system is found to increase with heat source temperature to 423 K for the first alloy pair and 433 K for the second alloy pair. Beyond which its effect is insignificant.

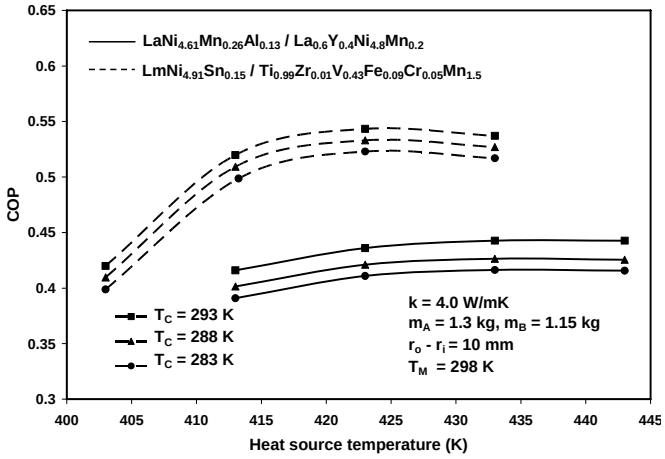


Figure 7. EFFECT OF T_H AND T_C ON COP

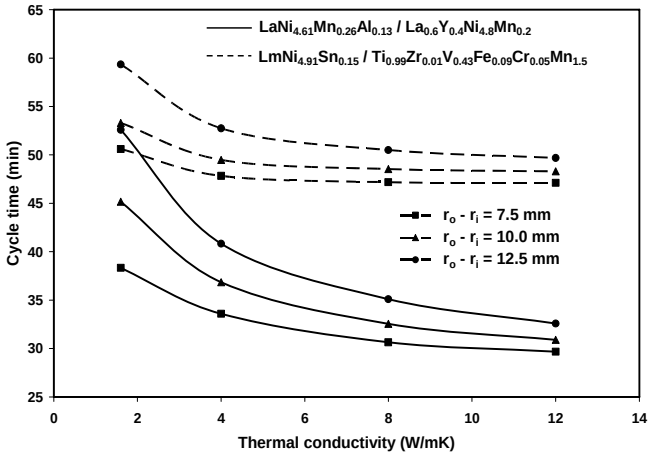


Figure 8. EFFECT OF THERMAL CONDUCTIVITY AND BED THICKNESS ON CYLCE TIME

Figs. 8 and 9 show the effect of thermal conductivity and bed thickness on the cycle time and specific cooling power. For a bed thickness of 7.5 mm, the cycle time decreases with increasing effective thermal conductivity up to 4 and 8 W/mK for first and second alloy pairs, respectively. Beyond this value no significant effect on the cycle time is observed. However, the bed thickness and the thermal conductivity are interrelated parameters. An optimum value of thermal conductivity is to be selected for a particular bed thickness. This result is very important from the system cost and efficiency point of view.

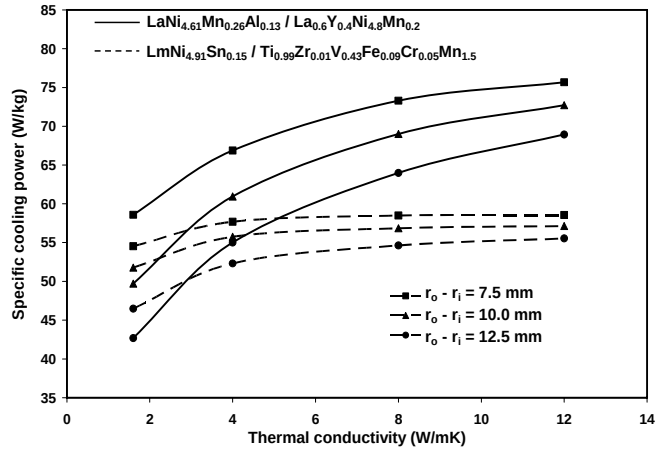


Figure 9. EFFECT OF THERMAL CONDUCTIVITY AND BED THICKNESS ON SCP FOR TWO ALLOY PAIRS

CONCLUSION

Performance analysis of the metal hydride cooling system working with $LmNi_{4.91}Sn_{0.15}$ / $Ti_{0.99}Zr_{0.01}V_{0.43}Fe_{0.09}Cr_{0.05}Mn_{1.5}$ and $LaNi_{4.61}Mn_{0.26}Al_{0.13}$ / $La_{0.6}Y_{0.4}Ni_{4.8}Mn_{0.2}$ has been carried out. The results show that the performance of the system can be controlled by optimizing the heat source, heat sink and refrigeration temperatures. However, these three temperatures depend upon the available heat sources, ambient temperature and cooling requirement. For the given operating temperatures of 423/298/293 K and 433/298/293 K, the COP and the specific cooling power of the single-stage, single-effect metal hydride cooling system are found to be 0.543, 53.25 W/kg and 0.43, 56.2 W/kg of alloy, respectively. Thin bed thickness is preferred for the shorter cycle time. A favorable value of effective thermal conductivity will improve the system performance significantly.

REFERENCES

[1] Ram gopal, M., and Srinivasa Murthy, S., 1995. "Performance of a metal hydride cooling system". *Int J Refrig,* **18**(6), July, pp. 413–420.

[2] Ram gopal, M., and Srinivasa Murthy, S., 1999. "Experiments on a metal hydride cooling system working with ZrMnFe/$MmNi_{4.5}Al_{0.5}$ pair". *Int J Refrig,* **22**(2), March, pp. 137–149.

[3] Fedorov, E.M., Shanin, Y.I., and Izhvanov, L.A., 1999. "Simulation of hydride heat pump operation". *Int J Hydrogen Energy,* **24**(10), October, pp. 1027–1032.

[4] Jang, K.J., Fateev, G.A., Park, J.G., Han, S.C., Lee, P., and Lee, J.Y., 2001. "Simulation of the metal hydride heat pump system with the single and double reactors". *Int J Hydrogen Energy,* **26**(3), March, pp. 237–241.

[5] Qin, F., Chen, J., Lu, M., Chen, Z., Zhou, Y., and Yang, K., 2007. "Development of a metal hydride refrigeration system as an exhaust gas-driven automobile air conditioner". *Renewable Energy,* **32**(12), October, pp. 2034–2052.

[6] Ni, J., and Liu, H., 2007. "Experimental research on refrigeration characteristics of a metal hydride heat pump in auto air-conditioning". *Int J Hydrogen Energy,* **32**(13), September, pp. 2567–2572.

[7] Payá, J., Linder, M., Laurien, E., and Corberán, J.M., 2009. "Dynamic model and experimental results of a thermally driven metal hydride cooling system". *Int J Hydrogen Energy,* **34**(7), April, pp. 3173–3184.

[8] Inproceedings of Hydrogen and Hydrogen Storage - Methods and Materials, 2009. Linder, M., and Laurien, E., "Thermally driven sorption machine for fast hydrogen exchange". IISc Bangalore, pp. 128. Paper number 54.

[9] Mellouli, S., Askri, F., Dhaou, H., Jemni, A., and Ben Nasrallah, S., 2009. "Parametric studies on a metal-hydride cooling system". *Int J Hydrogen Energy,* **34**(9), May, 3945 – 3952.

[10] Satheesh, A., Muthukumar, P., and Dewan, A., 2009. "Computational study of metal hydride cooling system". *Int J Hydrogen Energy,* **34**(7), April, pp. 3164–3172.

[11] Inproceedings of National Conference on Refrigeration and Air Conditioning, 2009. Satheesh, A., Muthukumar, P., and Dewan, A., "Modelling of metal hydride based cooling system". IIT Madras, pp. 6.1. Paper number 49.